



Crystallization between (100) Goethite and (001) Orientation of Hematite – A Review

Ming Kuang Wang · Puu-Tai Yang ·
Tsung-Ju Chuang · C. Chachi Ou · Shan Li Wang

Accepted: 29 May 2023 / Published online: 2 August 2023
© The Author(s), under exclusive licence to The Clay Minerals Society 2023

Abstract The purposes of this study were: (1) to review the preparation and characterization of the intergrowth between goethite and hematite crystals; and (2) to propose a schematic diagram of the epitaxial relationships among three sets of (100) goethite twin crystals associated with the (001) orientation of the hexagonal prism of hematite. The $\text{Fe}(\text{ClO}_4)_3$ solution was prepared and aged at 70°C , which precipitated goethite initially and produced hematite later with prolonged aging. Goethite and hematite aged for 20 days were observed as star-shaped and hexagonal prisms, respectively. The results suggest that hematite could form later using goethite as a template surface. A selected area electron diffraction (SAED) pattern showed the epitaxial relationship among three sets of (100) goethite intergrowth crystals and hexagonal prisms with the (001) orientation of hematite. Goethite can be produced as lath-, X-, K-, or star-shaped crystals on the (100) orientation, depending on the $\text{Fe}(\text{ClO}_4)_3$ concentrations and the addition of HClO_4 to Fe

solution samples which were aged for a prolonged period at room temperature. The initial solubility products $[(\text{Fe}^{3+})(\text{OH}^-)^3]$ of the sample solution, rather than the nature of the nuclei, are the key factors governing the formation of goethite or hematite. The addition of acids and high concentrations of iron solutions extend the secondary hydrolysis and induction period (IP) and favor the formation of hematite. The index of the SAED pattern of the star-shaped goethite intergrowth twin crystal has a (100) plane parallel to this basal plane and rotates at a 60° angle between two or three sets of lath-shaped goethite crystals, which share the (011) plane and form goethite twins with ‘interpenetrated’ crystal growth. Stereoscopic viewing using Oak Ridge Thermal Ellipsoid Plot (ORTEP) and *CrystalMaker* software was deployed to explore the relationship and configuration of oxygen atoms between pseudo-hexagonal (100) goethite associated with hexagonal (001) hematite lattice planes. A schematic diagram of the epitaxial relationship between star-shaped (100) goethite, which is acting as a template facilitating later precipitation of (001) hexagonal prisms of hematite on it, is presented.

Associate Editor: Binoy Sarkar.

M. K. Wang (✉) · P.-T. Yang · T.-J. Chuang · S. L. Wang
Department of Agricultural Chemistry, National Taiwan
University, Taipei, Taiwan 106
e-mail: mkwang@ntu.edu.tw

C. C. Ou
Department of Chemical and Materials Engineering,
National University of Kaohsiung, Kaohsiung, Taiwan 811

Keywords Bright and dark field images · Crystal model · Epitaxy · Goethite twins · High resolution transmission electron microscopy (HRTEM) · Induction period (IP) · Selected area electron diffraction (SAED) · Solubility products

Introduction

Goethite and hematite are common constituents in lateritic soils, sediments, and rocks (Berner, 1969). Goethite and hematite crystals are based on hexagonal closest-packed (hcp) oxygen lattices. The stacking sequence repeats every two layers (ABAB—); in hematite, Fe^{3+} cations occupy one-half to two-thirds of the available octahedral sites. Channels are formed by the rows of empty sites and are occupied by protons of the two hydroxyl groups in goethite. Goethite ($\alpha\text{-FeOOH}$) has an orthorhombic unit cell with the axes $a=4.608 \text{ \AA}$, $b=9.956 \text{ \AA}$, and $c=3.021 \text{ \AA}$ (Schwertmann & Taylor, 1989) and belongs to the space group $Pbnm$ (#62), with four repeat formula units per unit cell (Ghose et al., 2009; Gonzalez et al., 2000). The position of Fe^{3+} cations in hematite repeats every three layers (ABCABC—); the unit cell (i.e. the c axis in the hexagonal crystal system) corresponds to a six-layer period (Gonzalez et al., 2000). Hematite ($\alpha\text{-Fe}_2\text{O}_3$) has a hexagonal unit cell with $a=5.034 \text{ \AA}$ and $c=13.752 \text{ \AA}$ (Schwertmann & Taylor, 1989) and space group $R\bar{3}c$ (#167), with six formula units per unit cell (Gonzalez et al., 2000).

Several different methods are used to prepare goethite and hematite. Goethite can be prepared from an Fe^{3+} system, including alkaline or acid or cysteine/2-line ferrihydrite from Fe^{2+} system, which produces acicular or lath-shaped goethite. Hematite can be prepared from the fast hydrolysis of $\text{Fe}(\text{NO}_3)_3 \cdot 9 \text{ H}_2\text{O}$ in HNO_3 acid, $\text{FeCl}_3 \cdot 6 \text{ H}_2\text{O}$ salt with HCl , or $\text{Fe}(\text{ClO}_4)_3 \cdot 9 \text{ H}_2\text{O}$ near 100°C , from which diamond-shaped unidimensional crystals of 70–100 nm were observed (Cornell & Schwertmann, 2003; Schwertmann & Cornell, 2000). Hematite prepared from 2-line ferrihydrite formed small platelets or spindle-type crystals. The ferrihydrite was named by Chukhrov et al. (1973). In addition to the previous methods, crystalline $\alpha\text{-FeOOH}$ (i.e. lath and twining goethite) can be prepared by four methods: (1) a 0.001 M $\text{Fe}(\text{ClO}_4)_3$ with $\text{NaHCO}_3/\text{Fe}=0.25$ solution aged at room temperature for 10 y formed lath- and star-shaped goethite; (2) 0.01 M $\text{Fe}(\text{ClO}_4)_3$ and 0.0002 M HClO_4 solutions were aged at room temperature for 13 y and produced star-shaped goethite; (3) 0.05 M $\text{Fe}(\text{ClO}_4)_3$ solution aged at room temperature for 14 y formed K- and X-shaped intergrowth of goethite (Hsu, 1973; Hsu & Marion, 1985; Wang, 1987); and (4) acicular and

star-shaped goethite were prepared at pH (12–13) and heated at 70°C for up to 72 h (Atkinson et al., 1968; Barron et al., 1997; Cornell & Mann, 1983; Cornell & Schwertmann, 2003; Schwertmann & Cornell, 2000).

Earlier research reports indicated that the formation of $\alpha\text{-FeOOH}$ and $\alpha\text{-Fe}_2\text{O}_3$ can be determined by several factors: temperature, pH, Fe^{3+} concentration, anionic species, hydrolysis rate, nucleation, particle size, etc. Inconsistencies in the earlier literatures, however, indicated that these factors could be interrelated. Goethite and hematite were prepared at various temperatures between 5 and 165°C (Schwertmann & Cornell, 2000). While hematite was favored to form at higher temperatures and high $\text{Fe}(\text{ClO}_4)_3$ concentrations under acidic conditions; goethite was favored at low temperatures with low iron concentrations (Wang & Hsu, 1980).

In addition to the individual formation of goethite or hematite, transformation from goethite to hematite was evaluated in the following studies. Hematite is known to transform from goethite through dehydration (Naono et al., 1987; Weidler et al., 1998). The microstructure of hematite was studied by high-resolution electron microscopy (HRTEM) (Watari et al., 1979, 1983), which was formed by the dehydration of goethite. The topotactic relationship between goethite and hematite should be $(100)_G//(\text{001})_H$ (Van Oosterhout, 1960), where the directions [001], [100], and [010] of goethite became the directions [001], [010], and [210] of hematite. Due to the close relationship between the two crystalline structures, different slip mechanisms can be proposed favoring the phase transformation. Phase transformation into hematite particles was found to be epitaxial on goethite (Lin et al., 2014) and re-precipitation in the process of hematite formation (Cornell et al., 1974). The evolution of the microstructure of hematite derived from synthetic goethite over a wide temperature range ($400\text{--}1100^\circ\text{C}$) has been investigated systematically using powder X-ray diffraction (XRD) and transmission electron microscopy (TEM) (Kryukova et al., 1991). Based on the structure refinements of XRD patterns and TEM investigations, Jiang et al. (2000) illustrated that the non-uniform X-ray line broadening effect is caused by the plate-like shape of the hematite crystal. A phase transformation of synthetic goethite, heated above 250°C , led to the appearance of hematite (Saito et al., 2016).

Morphological changes when goethite transformed to hematite were also observed using TEM and HRTEM investigations. In situ analysis of mineral dehydroxylation, which was affected by the electron beam, was studied using HRTEM. The transformation of hematite from goethite has been discussed but the coexistence of goethite and hematite crystals and their intergrowth relationship have not previously been evaluated in depth.

The present study aimed to review how to prepare and characterize the intergrowth between goethite and hematite crystals, including how to improve the ability to interpret the SAED pattern of the crystal epitaxial relationship between three sets of (100) goethite twinning crystals associated with the (001) orientation of the hexagonal prism of hematite.

Materials and Methods

Formation of Goethite and Intergrowth of Goethite Crystals

Usually, goethite particles elongate in the [100] a direction, are needle-like, and contain intergrowths of goethite twins with varied shapes of the (210) plane. Goethite twins were precipitated from iron salt solutions at 25°C and pH 4, the product of which consisted of 2 or 3 lath-shaped goethite twins. The star-shaped goethite twins were prepared at $[\text{OH}^-]=0.3 \text{ mol L}^{-1}$ aged at 70°C. Epitaxial twins consist of a hematite center with outgrowths of acicular goethite. Large goethite twinning particles with well developed {101} and {210} terminal faces were reported by Schwertmann and Pfab (1994) as having produced vanadium goethite twinning. The 2-line ferrihydrite was observed as a result of production with addition of 0.3 M KOH and heated at 70°C (Schwertmann & Murad, 1983; Schwertmann et al., 2004). Polymeric star-shaped goethite twinning was produced in 0.3 M alkaline media aged at high temperature (i.e. 70°C), and is quite common along the a direction. Epitaxial goethite twins occurred (Cornell & Giovanoli, 1985; Schwertmann et al., 2004) and transformed from ferrihydrite (Chukhrov et al., 1973) in both acid and alkaline media. However, star-shaped goethite twins are produced only under high-pH conditions. Outgrowths of goethite developed in the [100] direction (a axis) and terminated in the [210]

faces due to phosphorus (P) adsorption (Barron et al., 1997). The (021) plane is a termination plane, which is parallel to the a axis of hematite; goethite (001) is parallel to the (001) plane of hematite. Different types of goethite twins can be predicted with variations in synthetic conditions (Atkinson et al., 1968).

Methods to Prepare the Intergrowth of Goethite and Hematite

Formation of Goethite and Hematite with Fe Solution Aged at 70°C

In general, the $\text{Fe}(\text{ClO}_4)_3$ with HClO_4 solutions can be prepared and aged at 70°C. The Fe solution samples were monitored for their hydrolysis and precipitates of Fe oxide during the aging period. The chemical determinations, including the H^+ and OH^- concentrations and solution pH, calculation of $(\text{Fe}^{3+})(\text{OH}^-)^3$ solubility products (K_{sp}), amorphous and total polymeric iron(III) hydroxides (%), XRD analysis, TEM and HRTEM investigations, bright and dark field imaging, and SAED patterns of particles were described in detail by Hsu (1973), Hsu and Wang (1980), Wang and Hsu (1980), and Wang et al. (1981). The chemicals were supplied by G.F. Smith Co. (Portland, Oregon, USA). The present study used 0.1 M $\text{Fe}(\text{ClO}_4)_3$ with and without the addition of HClO_4 (i.e. HClO_4/Fe molar ratio of $R=0, 0.6, 0.8$). A series of 0.004 M $\text{Fe}(\text{ClO}_4)_3$ solutions with R values of 4–10 aged at 70°C as examples were used to describe the Fe hydrolytic behavior and Fe oxide precipitates under the perchlorate acid system.

Results and Discussion

Hydrolytic Behavior of 0.1 M $\text{Fe}(\text{ClO}_4)_3$ Solution ($R=0, 0.6, 0.8$) Aged at 70°C

The initial pH, turbidity, and solubility products $(\text{Fe}^{3+})(\text{OH}^-)^3$ of the sample with $R=0$ were: 1.42, <0.1 JTU (Jackson Turbidity Unit), and $10^{-38.6}$, respectively. After a 6-h induction period (IP), the sample solution was aged at 70°C, and the solution turned rapidly from a clear solution (i.e. a light reddish color) into a turbid suspension, began secondary hydrolysis and polymerization, and gradually Fe precipitates were formed. Thus, hydrolytic products

of Fe precipitates settled to the bottom of the glass container. The pH values of Fe solution samples and amounts of polymeric 'Fe(III) hydroxides' decreased gradually the solution pH and increased polymeric 'Fe(III) hydroxides' with prolonged aging until 75% of the Fe(III) was polymerized (i.e. 20 days) (Hsu & Wang, 1980). Meanwhile, with $R=0.6$ or 0.8 in a $0.1 \text{ M Fe}(\text{ClO}_4)_3$ solution, the initial $(\text{Fe}^{3+})(\text{OH}^-)^3$ solubility products were close to $10^{-40.5}$ or $10^{-40.7}$, and increasing HClO_4 concentrations decreased the solution's initial and final pH and extended their IPs to 40 and 63 days, respectively. The XRD patterns of these Fe precipitates showed highly crystalline hematite only.

X-ray Analysis

Suspensions from the sample were collected for XRD analysis as soon as the Fe solution became turbid (i.e. 6 h) for the $0.1 \text{ M Fe}(\text{ClO}_4)_3$ solution ($R=0$) aged at 70°C . The XRD analysis showed the d spacings for goethite at 2.44, 2.58, 2.69, and 4.18 \AA . Then, the Fe solution began to appear polymerized shortly after the IP of the secondary hydrolysis; the d spacings of hematite at 2.51, 2.69, and 3.67 \AA and the amount of hematite increased gradually with prolonged aging (Hsu & Wang, 1980). The initial XRD reflection peak intensities of goethite were relatively weak compared to the reflection peak intensities of hematite after 20 days of aging, but no further change in relative goethite and hematite XRD reflection peak intensities was observed after the same amount of time. This result indicated that hematite was the only major product developed at the later aging stage. Thus, goethite precipitates formed first, and hematite formed later.

For the initial solubility products $[(\text{Fe}^{3+})(\text{OH}^-)^3]$ of a sample solution, K_{sp} is a key factor in the final hydrolytic precipitates of $\alpha\text{-FeOOH}$ and $\alpha\text{-Fe}_2\text{O}_3$ (Hsu, 1973; Hsu & Marion, 1985). Based on the K_{sp} of goethite and hematite, the relative abundance of Fe-oxide species should be interpreted as being governed by the solution $(\text{Fe}^{3+})(\text{OH}^-)^3$ solubility products with respect to the K_{sp} of goethite and hematite (i.e. K_{sp} close to 40 and 42), respectively. Schematic demonstration of the impact of the initial solution solubility products $[(\text{Fe}^{3+})(\text{OH}^-)^3]$ on the development of goethite and hematite with respect to their K_{sp} values was illustrated in detail earlier (Hsu & Wang, 1980).

TEM Investigations

For the TEM investigations, samples were collected from the $0.1 \text{ M Fe}(\text{ClO}_4)_3$ solution ($R=0$) aged at 70°C . A suspension sample aliquot was diluted to the Fe concentration of $\sim 0.02\%$; then, the precipitates were dispersed by ultrasonication. A Siemens Model I transmission electron microscope (Berlin, Germany) was used for this study. A drop of Fe suspension was placed onto a copper grid (3.05 mm in diameter, 300 mesh), coated with formvar film and dried at 25°C .

TEM images of samples collected from the $0.1 \text{ M Fe}(\text{ClO}_4)_3$ solution ($R=0$) aged at 70°C for 1 day contained various amounts of lath- and star-shaped goethite particles (i.e. $0.5 \mu\text{m}$ in size), which were overlain by poorly hexagonal-shaped plates of hematite (Hsu & Wang, 1980). Hexagonal plates of hematite covered nearly all lath-shaped and star-shaped goethites and increased in quantity after Fe solution aging for 20 days (Hsu & Wang, 1980). The existence of lath- or star-shaped goethite and hexagonal plates of hematite has been well documented after a 20-day aging period with no significant change. This result suggests the formation of goethite in the early hydrolytic stages and hematite in the later stage of the aging period, and goethite acts as a template surface to be overlain by a hexagonal hematite prism at a later stage. The relative proportions of $\alpha\text{-FeOOH}$ and $\alpha\text{-Fe}_2\text{O}_3$ are governed mainly by the solution environments, especially the initial $(\text{Fe}^{3+})(\text{OH}^-)^3$ solubility products and Fe solution pH, with respect to the K_{sp} values of goethite and hematite, instead of the speciation of nuclei. Hematite was suggested to act as a nucleus for the formation of goethite, but no evidence was provided in support of this assertion (Wefers, 1966).

Hydrolytic Behavior of $0.004 \text{ M Fe}(\text{ClO}_4)_3$ Solutions Aged at 70°C

A series of $0.004 \text{ M Fe}(\text{ClO}_4)_3$ solution samples with various R values of 4–10 and aged at 70°C was studied. The addition of HClO_4 decreased the initial pH and amount of $(\text{Fe}^{3+})(\text{OH}^-)^3$ solubility products and extended its secondary hydrolysis and IP. For example, with the addition of HClO_4 concentrations of $R=4$ –10, the initial solution pH decreased from 1.79 to 1.38, and the final (i.e. aged for 111 days) solution pH decreased from 1.49 to 1.20. The IP of

these Fe solutions extended from 6 h to 19 days. The K_{sp} values increased from 39.3 to 40.4, and amorphous Fe(III) hydroxide (%) and total polymeric Fe(III) hydroxide (%) decreased from 0.35 to 0.08 and from 99.5 to 93, respectively, with respect to the initial and final aging periods (i.e. 111 days) (Hsu & Wang, 1980). After the secondary hydrolysis and polymerization were initiated and reached equilibrium, ~99% of the total polymeric Fe(III) hydroxide $R=4, 6, 8,$ or 10 samples and 93% of the total Fe(III) were observed in all samples throughout the polymerization process. All sample solutions progressed rapidly and reached equilibrium. The final $(\text{Fe}^{3+})(\text{OH}^-)^3$ solubility product was calculated to be $\sim 10^{-42}$. The XRD patterns showed that both goethite and hematite were present, but hematite had a more intense XRD reflection than that of goethite, and it increased with increasing HClO_4 concentrations. The TEM images also showed that the hexagonal prism of hematite grew on top of star-shaped goethite (Fig. 1a, b). The other type of hematite particles appeared to be irregular hexagonal plates with four sides of equal length and two shorter sides (Fig. 1b). These species of intergrowth of goethite and hematite particles also increased markedly with increasing addition of HClO_4 and prolonged aging at 70°C (i.e. 111 days).

HRTEM Investigations and SAED Patterns

Representative particles of star-shaped goethite overlain by hexagonal prisms (i.e. hematite) were investigated by HRTEM (JEM 200-kV, Tokyo, Japan). The HRTEM sample preparation was approximately identical to that of TEM, but the sample was coated with a carbon film and dried at room temperature. The HRTEM investigations included both bright- and dark-field images, and SAED patterns of star-shaped goethite particles overlain with the hexagonal prism of hematite were reported by Wang et al. (1981). These goethite crystals had identical SAED patterns except for the difference in diffraction spot intensity. The index of the SAED pattern and TEM images of the star-shaped goethite twin crystal had a (100) plane. Two sets of lath-shaped goethites formed as X-shaped goethite twin crystal and have included angles at 60° and 120° , and shared with (011) plane. The bright- and dark-field images further support the interpretation of three sets of goethite formed a

star-shaped goethite twin on the same plane and not on the stacking arrangement of the intergrowth of goethites.

For further study, a 0.004 M $\text{Fe}(\text{ClO}_4)_3$ and 0.04 M in HClO_4 solution ($R=10$) aged at 70°C was prepared. The reaction products were goethite and dominant hematite (Hsu & Wang, 1980). Transmission electron micrographs also showed that the hematite in this 0.004 M $\text{Fe}(\text{ClO}_4)_3$ solution sample ($R=10$) observed two different growth habits: an irregular hexagonal plate of hematite particles appeared to have four sides of equal length and two considerably shorter sides. The second type of particle appeared to be a hexagonal plate of hematite underlain by star-shaped goethite (Fig. 2a); the SAED pattern of this particle is presented in Fig. 2b.

The simplest interpretation assumes the specimen to be composed of the (001) orientation of hematite and three lath-shaped (i.e. star-shaped) intergrowths of goethite crystals in the (100) orientation, to have a 60° angle between three neighboring lath-shaped goethite crystals. This is based on the ideal electron diffraction patterns for the (100) goethite and (001) hematite (Hirsch et al., 1977). The indexed SAED pattern shows that the hematite crystal has a basal plane (001) parallel to the micrograph and diffraction pattern (Fig. 2c). The diffraction spots nearest to the origins were indexed to be (020) and $(0\bar{2}0)$, which relate to the 4.98 Å basal spacing of goethite (JCPDS 17–536). A composite of the hematite diffraction patterns is shown in Fig. 2b. The six peripheral diffraction spots are indexed as (061), 1.453 Å of goethite associated with (300), 1.452 Å of hematite, and the middle sets of six diffraction spots refer to (021), 2.58 Å of goethite associated with (110), 2.51 Å of hematite (JCPDS 13–534) (Fig. 2b, c). Each of the three sets of lath-shaped goethite crystals has its (100) plane parallel to this basal plane and rotated at a 60° angle and is associated with (001) hematite (Fig. 2d). This is only a simple interpretation of the SAED pattern, which illustrated the relationship between goethite and hematite and its crystal growth. Furthermore, this interpretation is consistent with the morphological observation of three lath-shaped goethites at a 60° angle radiating from the hexagonal vertices (i.e. hematite).

To verify the indexing of goethite and hematite, the SAED spots located nearest to the origins and indexed to goethite (020) were selected for

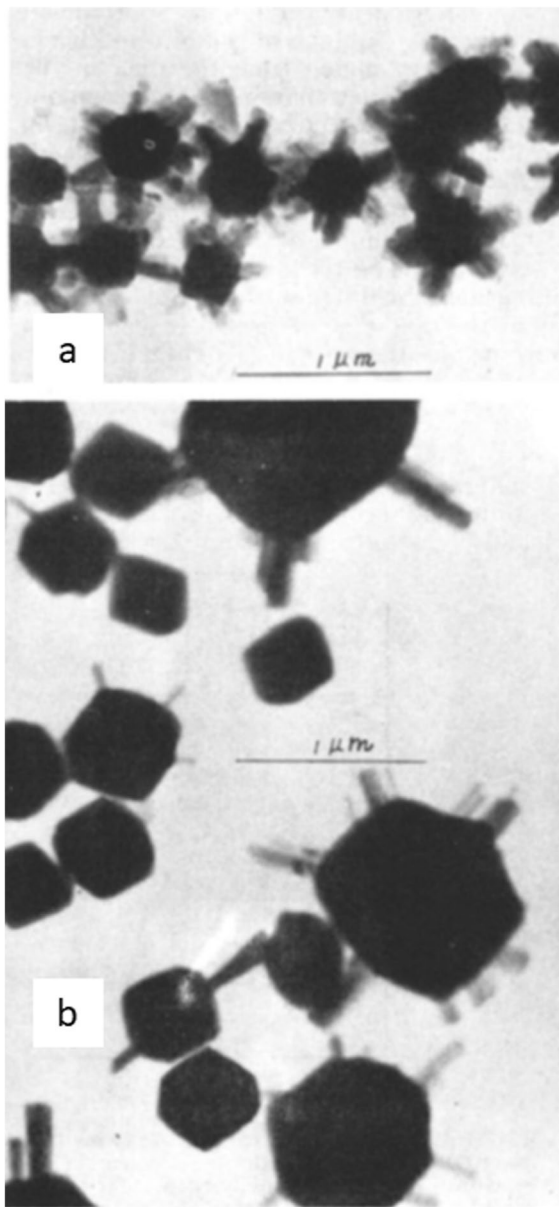


Fig. 1 TEM images of Fe oxide particles observed from three 0.004 M $\text{Fe}(\text{ClO}_4)_3$ solutions aged at 70°C for 111 days with **a** $R=6$ and **b** $R=8$ or 10

examination by dark field electron microscopic imaging. When the electron beam was directed to the (020) diffraction spot of goethite, most of the lath-shaped goethite crystals lit up, whereas the hexagonal plate (i.e. hematite) at the center remained dark (Fig. 2e). This observation further confirmed that the star-shaped goethite is quite stable under the HRTEM

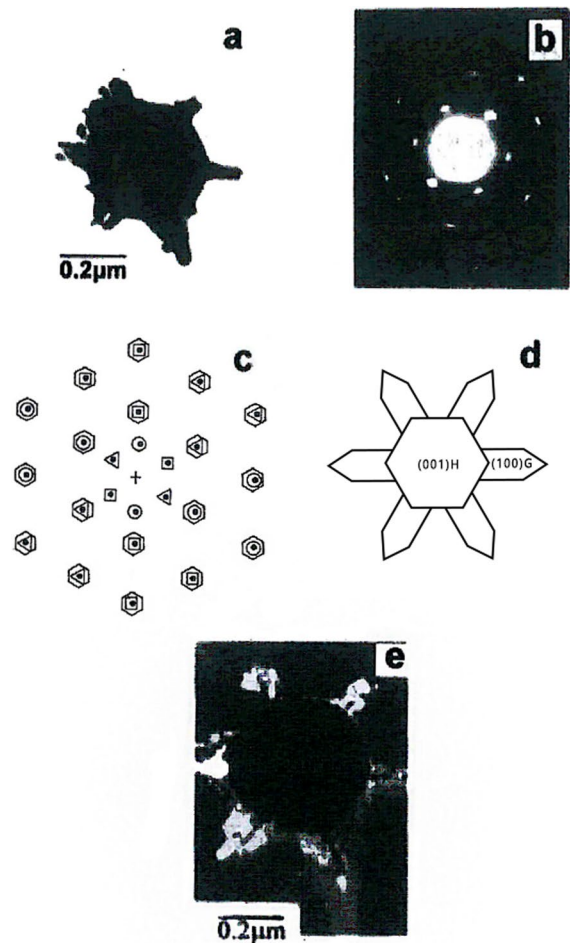


Fig. 2 TEM investigations of a hexagonal plate-shaped hematite grown on star-shaped goethite **a** with a bright field image. **b** SAED pattern of the hexagonal hematite plate grown on star-shaped goethite twinning crystals. **c** Indexing of the SAED pattern. \odot refers to hematite in the (001) orientation. \circ , Δ , and \square refer to three lath-shaped sets of goethite crystals in the (100) orientation, with 60° between neighboring pairs of goethite crystals in part **b**. **d** Each of three sets of lath-shaped goethite crystals has its (100) plane parallel to this basal plane and rotated at 60°, which is associated with the (001) plane of hexagonal-prism hematite. **e** Dark field image of star-shaped goethite and hexagonal plate hematite, selected diffraction spot at (020) goethite; most of the lath-shaped goethite crystals lit up, whereas the hexagonal plate of hematite at the center remained dark

high-energy electron beam, which helps interpret its SAED pattern with double diffraction spots. The fact that only most of a lath-shaped goethite lit up in the dark field images indicates that the entire structure is highly defective. The SAED of the other irregular

hexagonal particles in Fig. 2b was indexed to be hematite in the (211) orientation (Wang et al., 1981).

Hematite grew preferentially with its hexagonal basal planes parallel to (100) goethite (Schwiersch, 1933). The intergrowth plane is an oxygen layer common to both lattices. The intergrowth of goethite and hematite was also demonstrated (Wefers, 1966). Wefers (1966) also suggested that hematite developed first and subsequently acted as a nucleus for the development of goethite. In highly supersaturated solutions, under equal growth conditions, goethite developed under hexagonal hematite (100) prism surfaces and star-shaped crystals. Nevertheless, Wefers (1966) did not present further experimental evidence of the progress of crystal growth. However, other authors clearly showed that goethite developed prior to hematite, and (100) goethite crystals radiated (star-shaped) under the (001) prism surface of the hexagonal hematite plate (Hsu & Wang, 1980; Wang et al., 1981).

The size of star-shaped goethite twins associated with hexagonal hematite is $\sim 0.5 \mu\text{m}$ (Figs. 1, 2), which is $< 1 \mu\text{m}$ and $> 0.2 \mu\text{m}$. SAED occurs as a hexagonal pattern (Fig. 2b, c). Thus, the twins exhibit pseudo-hexagonal symmetry with “interpenetrated” angles of $\sim 120^\circ$ and are not shown as “contact” twins (Cornell & Mann, 1983). According to Atkinson et al. (1968), Cornell and Mann (1983), and Barron et al. (1997), the (021) faces have the greatest concentration of connected hydroxyls and preferentially adsorbed phosphate and grew slowly, thus keeping the star arrows short relative to their crystal width, forming a terminated edge. It may be correlated with the formation of X-, K- and star-shaped goethite twins. The real mechanism of termination for the intergrowth of goethite twin crystals remains obscure and merits further, in-depth study.

Schematic Diagram of the Epitaxial Relationship between Three Sets of Intergrown (100) Goethite Crystals Associated with the (001) Orientation of Hexagonal Hematite Prisms

The proposed schematic diagram (Fig. 3) of the epitaxial relationship between three sets of (100) goethite crystals acting as a template onto which the (001) plane of hexagonal hematite prisms are overlaid shows a rectangular plane that represents goethite resting on the (100) plane. All oxygen atoms are located at $Z = \pm 1/4$ in hematite and at $X = \pm 1/4$ in

goethite. The goethite lath axis is generally understood to lie parallel to the z axis. Thus, the proposed scheme implies that the z axis of goethite bisects the angle between the a_1 and $-a_3$ axes of hematite. Lath-, X-, K-, and star-shaped goethite crystals were prepared and examined. The results indicated that the three sets of lath-shaped goethite crystals are planar, and the model proposes that epitaxial crystal growth of the (001) plane of hematite formed later and overlaid the (100) goethite surface plane.

Recently, the stereoscope viewer, Oak Ridge Thermal Ellipsoid Plot (*ORTEP*), and *CrystalMaker* software were deployed for further study of the epitaxial relationship between (100) goethite and (001) hematite and to assess the correctness of Fig. 3. The *ORTEP* is a software program used for the visualization and analysis of crystal structures and was developed by the Oak Ridge National Laboratory (ORNL), Tennessee, USA. *CrystalMaker* is a software program that is designed to help scientists visualize and manipulate crystal structures in 3D and was developed by *CrystalMaker* Software Limited, Oxford, UK.

Crystallographic data of goethite and hematite obtained from the American Mineralogist Crystal Structure Database (AMC, cif) was input into *ORTEP* or *CrystalMaker* software. A pseudo-hexagonal oxygen was shown on the (100) orientation of goethite

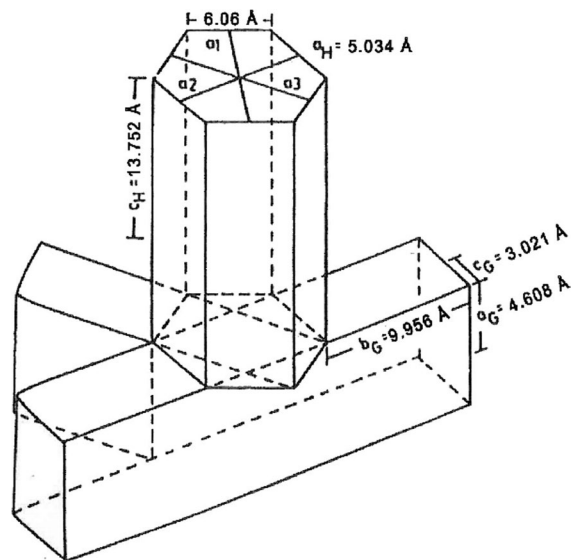


Fig. 3 Schematic diagram of the epitaxial relationships among three sets of the (100) orientations of goethite and (001) hexagonal prisms of hematite

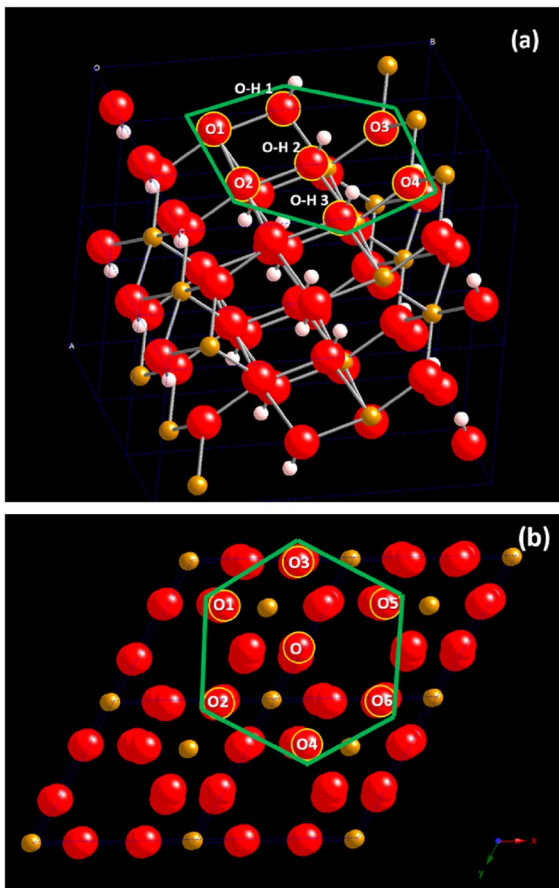


Fig. 4 The configuration of pseudo-hexagonal oxygen on the **a** (100) goethite and **b** hexagonal (001) hematite lattice planes

and a hexagonal oxygen on the (001) orientation of hematite (Fig. 4a, b). The atom positions and other atomic information for (100) goethite and (001) hematite lattice planes are listed in Table 1. All of the atom positions and atomic information, including

distances and angles of the pseudo-hexagonal oxygen on the goethite (100) lattice plane, are quite different from the hexagonal oxygen on the hematite (001) lattice plane (Table 2).

The area of pseudo-hexagonal oxygen of goethite is 12.48 \AA^2 , which is much smaller than that of hexagonal oxygen of hematite (i.e. 18.02 \AA^2) (Table 2). No atom positions or atomic information (i.e. distances and angles) of the pseudo-hexagonal (100) goethite coincided with those of hexagonal (001) hematite lattice planes. The inference is, thus, that $\text{Fe}(\text{ClO}_4)_3$ and the addition of HClO_4 aged at 70°C for 20 days consisted of star-shaped intergrowths of goethite overlain by hexagonal prisms of hematite particles. The epitaxial relationship among the three sets of (100) goethite formed at the initial aging stage, and then the Fe solubility product in solution decreased slowly as the hexagonal (001) orientation of hematite was formed. The star-shaped (100) goethite crystals act as template surfaces; the hexagonal prism represents hematite (001) overlaid on the (100) goethite surface plane (Figs. 1, 2a, d, e). This may have been caused by the highest concentration of Fe connected with singly coordinated hydroxyls along the pseudo-hexagonal (100) goethite lattice plane (Fig. 4a, i.e. OH1 and OH3).

Conclusions

Goethite crystals can be formed as lath-, X-, K-, or star-shaped on the (100) orientation with various concentrations of $\text{Fe}(\text{ClO}_4)_3$ and the addition of HClO_4 solution in samples aged at room temperature for a long period of time. Two or three sets of the lath-shaped goethite shared the (011) plane to

Table 1 Atom positions (unit distances) of pseudo-hexagonal oxygen on goethite (100) and hexagonal hematite (001) lattice planes

Goethite (100)				Hematite (001)			
Atom	x axis	y axis	z axis	Atom	x axis	y axis	z axis
O1	0.21	0.30	0.75	O1	0.36	0.33	0.08
O2	0.21	0.30	1.75	O2	0.67	1.03	0.08
O-H 1	0.30	0.55	0.25	O3	0.67	0.03	0.08
O-H 3	0.30	0.55	2.25	O4	1.36	1.33	0.08
O3	0.29	0.80	0.75	O5	1.36	0.33	0.08
O4	0.29	0.80	1.75	O6	1.67	1.03	0.08

Table 2 Atomic information for pseudo-hexagonal oxygen on goethite (100) and hexagonal hematite (001) lattice planes

Goethite (1 0 0)				Hematite (0 0 1)			
Atom	Atomic distance (Å)	Atom	Atomic angle (°)	Atom	Atomic distance (Å)	Atom	Atomic angle (°)
O1–O2	3.018	O1–O2–OH3	120.643	O1–O2	3.035	O1–O2–O4	112.168
O2–OH3	2.960	O2–OH3–O4	117.083	O2–O4	3.035	O2–O4–O6	123.916
OH3–O4	2.892	OH3–O4–O3	121.453	O4–O6	2.669	O4–O6–O5	123.916
O4–O3	3.018	O4–O3–OH1	121.453	O6–O5	3.035	O6–O5–O3	112.168
O3–OH1	2.892	O3–OH1–O1	117.083	O5–O3	3.035	O5–O3–O1	123.916
OH1–O1	2.960	OH1–O1–O2	120.643	O3–O1	2.669	O3–O1–O2	123.916

Areas of pseudo-hexagonal oxygen of goethite and hematite are 12.48 \AA^2 and 18.02 \AA^2 , respectively

form goethite twins with ‘interpenetrated’ crystal growth. Appropriate concentrations of $\text{Fe}(\text{ClO}_4)_3$ and the addition of HClO_4 solution, followed by aging at 70°C for 20 days produced star-shaped goethite intergrowth, which was overlain by hexagonal prisms of hematite particles. The epitaxial relationships among three sets of (100) goethite and the (001) orientation of the hexagonal prism of hematite was constructed. The schematic diagram shows that hexagonal prisms represent hematite resting on its (001) orientation, which is overlain on the (100) star-shaped goethite, which acts as a template surface plane. The mechanism of termination of the formation of X-, K-, and star-shaped goethite twins is not well known and merits further, in-depth study.

Acknowledgements The authors thank the Department of Agricultural Chemistry, National Taiwan University, for logistical support and laboratory assistance. They also thank Mr Wei Lin Liu, Department of Agricultural Chemistry, NTU and Professor C. Chachi Ou who operated the stereoscope viewer software *ORTEP* and *CrystalMaker* to explore the configuration of oxygen atoms on the pseudo-hexagonal (100) goethite and hexagonal (001) hematite lattice planes. Special thanks also to Professor Y.M. Chen of the same department for his technical assistance. The authors dedicate this paper to Professors P.H. Hsu, Rutgers University, New Brunswick, New Jersey, USA and K.H. Houng, National Taiwan University, Taipei, Taiwan.

Authors’ Contributions All authors contributed to the study conception and design. Material preparation, data collection, data analysis and revision of figures were performed by Ming Kuang Wang, Puu-Tai Yang, Tsung-Ju Chuang, C. Chachi Qu and Shan Li Wang. The first draft was prepared by Professor Ming Kuang Wang, helped by Professor C. Chachi Ou. All authors commented on drafts of the manuscript and approved the final version.

Funding Not applicable.

Data Availability The datasets used and/or analyzed during the current study are available from the corresponding author on reasonable request.

Declarations

Ethics Approval and Consent to Participate Written informed consent for publication of this paper was obtained from all authors. The manuscript does not report on or involve the use of any animal or human data or tissue. A copy of the written consent is available for review from the Editor-in-Chief of this journal.

Competing Interests The authors declare that they have no known competing financial interests or personal relationships that could have appeared to influence the work reported in this paper.

References

- Atkinson, R. T., Posner, A. M., & Quirk, J. P. (1968). Crystal nucleation in Fe(III) solutions and hydroxide gels. *Journal of Inorganic Nuclear Chemistry*, 30, 2371–2381.
- Barron, V., Galves, N., Hochella, M. F., Jr., & Torrent, J. (1997). Epitaxial intergrowth of goethite and hematite synthesized in phosphate media: A scanning force and transmission electron microscopy study. *American Mineralogist*, 82, 1091–1100.
- Berner, R. A. (1969). Goethite stability and the origin of red beds. *Geochimica Et Cosmochimica Acta*, 33, 269–274.
- Chukhrov, F. V., Zvyagin, B. B., Ermilva, L. P., & Gorshkov, A. I. (1973). New data on iron oxides in the weathering zone. *Proceedings of the International Clay Conference, Madrid, Spain, 1*, 397–404.

- Cornell, R. M., & Giovanoli, R. (1985). Effect of solution conditions on the proportion and morphology of goethite from ferrihydrite. *Clays and Clay Minerals*, *33*, 557–564.
- Cornell, R. M., & Mann, S. (1983). A high-resolution electron microscopy examination of domain boundaries in crystals of synthetic goethite. *Journal of Inorganic and Nuclear Chemistry*, *79*, 2679–2684.
- Cornell, R. M., & Schwertmann, U. (2003). *The Iron Oxides: Structures, Properties, Reactions, Occurrence and Uses* (2nd ed., p. 664). VCH, Verlag, GmbH, Weinheim.
- Cornell, R. M., Posner, A. M., & Quirk, J. P. (1974). Crystal morphology and the dissolution of goethite. *Journal of Inorganic and Nuclear Chemistry*, *6*, 1937–1946.
- Ghose, S. K., Waychunas, G. A., Trainor, T. P., & Eng, P. J. (2009). Hydrated goethite (α -FeOOH) (100) interface structure: Order water and surface functional group. *Geochimica Et Cosmochimica Acta*, *74*, 1943–1953.
- Gonzalez, G., Sagarazu, A., & Villalba, R. (2000). Study of the mechano-chemical transformation of goethite to hematite by TEM and XRD. *Materials Research Bulletin*, *35*, 2295–2308.
- Hirsch, P. A., Howie, R. B., Nicholson, D. W., & Whelan, M. J. (1977). *Electron microscopy of thin crystals*. Krieger Publishing, New York.
- Hsu, P. H. (1973). Appearance and stability of hydrolyzed $\text{Fe}(\text{ClO}_4)_3$ solutions. *Clays and Clay Minerals*, *21*, 267–277.
- Hsu, P. H., & Marion, G. (1985). The solubility products of goethite. *Soil Science*, *40*(2), 344–351.
- Hsu, P. H., & Wang, M. K. (1980). Crystallization of goethite and hematite at 70°C. *Journal of the Soil Science Society America*, *44*(1), 143–148.
- Jiang, J. Z., Stahl, K., Nielsen, K., & Costa, G. M. (2000). Anisotropic X-ray line broadening in goethite-derived haematite. *Journal of Physics Condensed Matter*, *12*, 4893–4898.
- Kryukova, G. N., Tsybulya, S. V., Solovyeva, L. P., Sadykov, V. A., Litvak, G. S., & Andrianov, M. P. (1991). Effect of heat treatment on microstructure evolution of hematite derived from synthetic goethite. *Materials Science and Engineering*, *A149*, 121–127.
- Lin, M., Liang, T., Lim, T., Meeling, C., Zhang, J., Tan, H. R., & Shiqiang, B. (2014). Hydrothermal synthesis of octahedral hematite (α - Fe_2O_3) nanoparticles: An epitaxial growth from goethite (α -FeOOH). *The Journal of Physical Chemistry*, *118*, 10903–10910.
- Naono, H., Nakai, K., Sueyoshi, T., & Yagi, H. (1987). Porous texture in hematite derived from goethite: Mechanism of thermal decomposition of goethite. *Journal of Colloid and Interface Science*, *120*, 439–450.
- Saito, G., Kunisada, Y., Nomura, T., Sakaguchi, N., & Akiyama, T. (2016). Twin formation in hematite during dehydration of goethite. *Physics and Chemistry of Minerals*, *43*, 749–757.
- Schwertmann, U. & Cornell, R. M. (2000). *Iron Oxides in the Laboratory – Preparation and Characterization*. (2nd ed., p. 188). VCH, Verlag, GmbH, D-69469, Weinheim.
- Schwertmann, U., & Murad, E. (1983). Effect of pH and formation of goethite and hematite from ferrihydrite. *Clays and Clay Minerals*, *31*, 277–284.
- Schwertmann, U., & Pfab, G. (1994). Structural vanadium in synthetic goethite. *Geochimica Et Cosmochimica Acta*, *58*, 4347–4352.
- Schwertmann, U., & Taylor, R. M. (1989). Iron oxides. Chapter 8. In J. B. Dixon & S. B. Weed (Eds.), *Minerals in Soil Environments* (pp. 379–438). Published by the Soil Science Society of America, Madison, WI.
- Schwertmann, U., Stanjek, H., & Becher, H.-H. (2004). Long-term in vitro transformation of 2-line ferrihydrite to goethite/hematite at 4, 10, 15 and 25°C. *Clay Minerals*, *39*, 433–438.
- Schwietersch, R. (1933). Thermischer abbau der natürlichen hydroxide des aluminums und dreierwertigen Eisen. *Chemie Der Erde*, *8*, 252–315.
- Van Oosterhout, G. (1960). Morphology of synthetic sub-microscopic crystals of [alpha] and [gamma] FeOOH and [gamma] Fe_2O_3 preparation from FeOOH. *Acta Crystallographica*, *13*, 932–935.
- Wang, M. K. (1987). Goethite twin arrangement and a goethite and hematite crystal intergrowth orientation model. *Journal of Chinese Agricultural Chemical Society*, *25*(4), 432–437.
- Wang, M. K., & Hsu, P. H. (1980). Effect of temperature and Fe(III) concentration on the hydrolytic formation of iron(III) oxyhydroxides and oxides. *Journal of the Soil Science Society of America*, *44*(5), 1989–1995.
- Wang, M. K., Greenhut, V. A., & Hsu, P. H. (1981). Electron microscopic study of hematite growth habits. *Soil Science*, *132*(1), 182–187.
- Watari, F., Delangnette, P., Van Landuyt, J., & Amelinckx, S. (1979). Electron microscopic study of dehydration and transformation. Part I. Twin formation and mosaic structure in hematite derived from goethite. *Journal of Solid State Chemistry*, *79*, 137–150.
- Watari, F., Delangnette, P., Van Landuyt, J., & Amelinckx, S. (1983). Electron microscopic study of dehydration and transformation. Part III. High resolution observation of the reaction processes FeOOH to α - Fe_2O_3 . *Journal of Solid State Chemistry*, *48*, 49–64.
- Wefers, K. (1966) Zum system Fe_2O_3 - H_2O , *Berichte Deutschen Keram. Gesellschaft*, *13*, 677–702 (in German, John Creer Library, Chicago).
- Weidler, P. G., Hug, S. J., Wetche, T. P., & Hiemstra, T. (1998). Determination of growth rates of (100) and (110) face of synthetic goethites by scanning force microscopy. *Geochimica Et Cosmochimica Acta*, *62*, 21–22.

Springer Nature or its licensor (e.g. a society or other partner) holds exclusive rights to this article under a publishing agreement with the author(s) or other rightsholder(s); author self-archiving of the accepted manuscript version of this article is solely governed by the terms of such publishing agreement and applicable law.